

Fracture mechanics analysis of coating/substrate systems

Part II: Experiments in bending

Sung-Ryong Kim^a, John A. Nairn^{b,*}

^aSam Yang R&D Center, 63-2 Whaam-Dong, Yusung-gu, Taejon, South Korea

^bMaterial Science and Engineering, University of Utah, Salt Lake City, Utah 84112, USA

Received 30 December 1998; received in revised form 2 December 1999; accepted 7 Decemeber 1999

Abstract

A series of coating/substrate systems with typical automotive finishes as coatings were loaded in four-point bending. The coatings in these specimens usually failed by multiple cracking; we recorded the density of coating cracks as a function of bending strain. These experimental results were fit to a new fracture mechanics theory of coating failure that predicts the next coating crack forms when the energy released by that fracture event exceeds the toughness of the coating. This fitting procedure led to experimental result for coating fracture toughness. We found that coating toughness continually dropped as the coatings were baked for longer times. There was also a profound substrate effect which means that coating fracture toughness must be regarded as an *in situ* toughness property. The toughness of polymeric coatings on steel substrates was more than an order of magnitude lower than the toughness of the same coating on polymeric substrates. The *in situ* coating toughness was also weakly dependent on coating thickness; it increased as the coating got thicker. © 2000 Elsevier Science Ltd. All rights reserved.

Keywords: Fracture Mechanics, Variational Mechanics, Coatings, Paints

1. Introduction

When coated or painted structures are subjected to short-term or long-term loads, or to thermal or moisture cycling, the first form a failure is often cracking of the coating layer [1–4]. Such cracking typically does not lead to structural failure, but it can represent functional failure of the coating. Coatings are usually intended to provide some function such as decoration (for paints), protection (for barrier coatings), or electrical properties (*e.g.* for insulation). Cracks in such coatings may ruin appearance (for paints), cease to protect (for barriers), or alter electrical properties. When designing coated structures and optimal coatings, it is important to be able to predict the conditions for which coating cracks form. It is also important to be able to characterize coatings to determine which coatings on which substrates will be the most resistant to cracking.

In some coating/substrate systems, coating cracks that form under axial loading become arrested at the coating/substrate interface. Continued loading leads to additional coating cracks or multiple cracking. Eventually, a roughly periodic array of coating cracks perpendicular to the loading direction develops [1–4]. In a previous paper [5] we analyzed coating fracture in straight-sided specimens subjected to axial loads using tensile loading or four-point bending. We proposed that multiple cracking failures under such loading can be analyzed by assuming that the next coating crack forms when the energy released due to the formation of that crack exceeds the fracture toughness of the coating [5]. We used a variational stress analysis to calculate the change in stresses due to formation of coating cracks and the energy released by such cracks. By equating the energy release rate to coating toughness and solving for strain, it is possible to predict the number or density of coating cracks as a function of applied strain.

*Corresponding author. Tel.: +1-801-581-3413; fax: +1-801-581-4816
E-mail address: john.nairn@m.cc.utah.edu (J. A. Nairn).

In this paper, we used the analysis of Ref. [5] to analyze experimental results for multiple cracking of typical coatings used as automotive finishes. The analysis of Ref. [5] considered both tensile loading and four-point bending. Experimentally, the four-point bending experiments worked much better and produced cleaner crack-density data than tensile loading experiments. All experiments described in this paper were for specimens loaded in bending. We found that the trends of most experiments conformed well to the fracture mechanics predictions of Ref. [5]. We were thus able to fit experimental results to theoretical predictions and determine the fracture toughness of coatings under various conditions. The fracture toughness always decreased as a function of baking time used to prepare the specimens. There was also a profound substrate effect. The *in situ* fracture toughness of these coatings was more than an order of magnitude lower on steel substrates than on polymeric substrates. We suggest that the coating toughness is controlled by the level of constraint placed on the coating by the substrate. Steel substrates constrain polymeric coatings. This constraint inhibits plastic deformation and makes the coating act like a brittle, low-toughness material. Similarly, the coating toughness increased slightly as the coating on steel substrates got thicker because the thicker coatings were constrained less than the thinner coatings.

2. Materials and Methods

2.1. Coatings

All coatings were supplied by the duPont Company. Two classes of coatings were used. One class of coatings was automotive clear-coat finishes that achieve final form by baking and chemical curing. The other class was a coating that consisted of low molecular weight polymer in various solvents; this coating achieves final form by solvent evaporation. The following coatings were used:

Coating A An automotive clear-coat finish (RKR35343) characterized as a high solids, rigid clear, one-component acrylic/melamine/silane coating (baked finish).

Coating B An automotive clear-coat finish (RKR35367) characterized as a high solids, rigid clear, one-component acrylic/melamine/silane coating (baked finish).

Coating C An automotive clear-coat finish (RK19004) characterized as a high solids, rigid clear, one-component acrylic/melamine clear coating (baked finish).

Coating D A solvent-evaporation finish (RC909) consisting of low molecular weight poly methyl-methacrylate (PMMA) in various solvents. This component has been used in automotive lacquers characterized as being brittle finishes. The viscosity average molecular weight of the PMMA in this coating was 75,000 g/mol.

The properties for these coatings are listed in Table I. In the remainder of this paper, the coatings are denoted by letters A, B, C, or D.

2.2. Substrates

Steel substrates 0.317 cm (1/8 inch) thick were supplied by the duPont Company already primed and coated with one of the four coatings (A through D). The primer layer was a 0.025 mm (1 mil) thick electrodeposited (ELPO) primer. The coatings were applied with thicknesses ranging from 0.152 to 0.304 mm (6 to 12 mils) and were pre-baked for 30 minutes at 130°C prior to shipping. The main function of the primer was to maximize adhesion to the coating. The mechanical properties of steel are listed in Table I. The steel modulus of 115000 GPa is an experimental results. It is lower than most common steel results. The modulus is only used to calculate coating toughness from experimental results. If a higher modulus was used in those calculations there would only be minor changes in the results; a higher modulus would lead to a slightly higher estimation of coating toughness. A list of all specimens tested with steel substrates is given in Table II.

Three types of polymeric substrates were used — polycarbonate (PC or General Electric's Lexan®), acrylonitrile-butadiene-styrene copolymer (ABS) and polyphenylene oxide/polystyrene blends (PPO/PS or Noryl®). PC was selected because its transparency made it easy to observe cracks in the coating layers. ABS and PPO/PS were selected because of their common use in automotive applications including applications

Table I. Material properties of the coatings and substrates. The moduli of the coatings and substrates were measured; the moduli of the coatings were measured after 24 hrs of baking at 130°C. The Poisson's ratios were taken from the literature, from product literature, or estimated.

Substrate or Coating	Modulus (MPa)	Poisson's Ratio
Coating A	1900	0.33 [†]
Coating B	2400	0.33 [†]
Coating C	1660	0.33 [†]
Coating D	1700	0.33 [†]
Steel	115000	0.28*
PC	2300	0.37*
ABS	2150	0.39*
PPO/PS	2550	0.40*

[†] Estimated value

* Product literature value

Table II. List of substrate and coating materials and thicknesses for the specimens tested.

Substrate	Thickness (mils)	Coating	Thickness (mils)
Steel	125	Coating A	6.0
Steel	125	Coating C	2.0
Steel	125	Coating C	2.0
PC	228	Coating A	4.5
PC	228	Coating B	4.0
PC	228	Coating C	6.75
PC	228	Coating D	6.0
ABS	259	Coating A	6.0
ABS	259	Coating D	7.8
Noryl [®]	375	Coating D	5.5

in which they are painted. The high T_g of PPO/PS makes it suitable for use with automotive finishes that require baking. The polymeric substrates were purchased from a plastic distributor in the form of extruded sheets. No primer was used with the polymeric substrates. The mechanical properties of the polymeric substrates are listed in Table I. A list of all specimens tested with polymeric substrates is given in Table II.

2.3. Sample Preparation and Experimental Setup

All metallic substrates were supplied by duPont already coated. The supplied samples had been baked slightly and had no initial cracks. These initial specimens also did not crack significantly during bending tests. In order to promote cracking, to study the effect of baking time, and to study effects of long-term aging qualitatively, all steel-substrate specimens were subjected to additional baking at 130°C.

For polymer substrates, the coatings were applied in our lab. Before applying the coatings, the polymer substrate surface was modified by grit blasting or by sanding with No. 600 sand paper. This surface modification was required to improve adhesion and reduce or eliminate substrate/coating delamination after the formation of coating cracks. The polymer substrate samples were subjected to various amounts of baking times. The baking temperatures had to be adjusted to accommodate the T_g of the substrate. The baking temperatures for PC, ABS, and PPO/PS substrates were selected to be 110°C, 60°C, and 130°C, respectively. Specimens with coating D (solvent-evaporation type coating) were baked at 60°C, as recommended

by duPont, to remove the solvents.

All specimens were straight sided 100 mm (4 inch) long and 12.5 mm (1/2 inch) wide. The steel specimens were machined to final dimensions. The polymer substrates were cut from already-coated polymer sheets. The specimens were first rough cut on a band saw and then milled to the final size using a pin router and a straight-edge specimen-shaped template. All specimens were tested in four point bending with a central span of 17 mm and total span of 51 mm between the outer-most loading points. The bending tests were done on a Material Testing System (MTS) Model 810 25 kN servo-hydraulic testing frame under displacement control mode at ambient temperature and humidity. Stress-strain data were collected using an IBM PC and custom developed software that interfaced the IBM PC to an MTS 464 Digital Display device. All experiments used a cross-head rate of 0.05 mm/s (0.118 inch/min).

Each specimen was loaded in four-point bending. As the test proceeded, the 17 mm central span area (the zone of constant bending moment in four-point bending) was examined for cracks. The coating cracks could be observed by eye and were recorded by pushing a button that superimposed a tick mark on the stress-strain data. After the experiment, the analysis software read the crack markings and reported number of cracks as a function of strain. The number of cracks divided by the central span length gave the crack density. We also recorded the entire stress-strain curve to see which cracks occurred in the linear elastic region and which occurred after substrate yielding.

With sufficiently thick coatings, it was easy to observe and mark cracks by eye. For some systems, the coating and substrate delaminated after the formation of one or a few coating cracks. When delamination occurred, it dominated failure and there were no additional coating cracks. This paper only presents data with multiple coating cracks or only results that were observed to have limited or no coating/substrate delamination.

2.4. Fracture Analysis

In a previous paper [5], we derived a fracture mechanics model for prediction of multiple crack formation during four-point bending experiments. In brief, we assumed that the next coating crack forms when the *total* energy release rate for the formation of that crack equals or exceeds the *in situ* fracture toughness of the coating. Using this assumption and a two-dimensional variational mechanics analysis, we showed that bending strain, ε_b , as a function of crack density, D , is

$$\varepsilon_b = -\frac{B}{2\bar{z}_1 E_c} \sqrt{\frac{G_{cc}}{C_3 t_c Y(D)}} - \frac{B \Delta \alpha \Delta T}{2\bar{z}_1 E_c C_1} \quad (1)$$

where B is the total specimen thickness, t_c is the thickness of the coating, and \bar{z}_1 is the position of the midpoint of the coating relative to the neutral axis of the beam. In the analysis, the z coordinate ranges from $-B/2$ to $B/2$ and the coating surface, or tensile-stress surface is at $z = -B/2$; the coating midpoint, \bar{z}_1 is thus $-(B - t_c)/2 - z_N$ where z_N (see below) is the z -coordinate of the neutral axis. E_c is the modulus of the coating, G_{cc} is the toughness or critical energy release rate of the coating, $\Delta \alpha = \alpha_c - \alpha_s$ is the difference in thermal expansion coefficients between the coating and the substrate, and $\Delta T = T_{test} - T_0$ is the difference in temperature between the test temperature and the stress-free temperature. The constants C_3 and C_1 and the $Y(D)$ function of crack density are a result of a variational mechanics analysis and depend only on the geometry of the specimen and the mechanical properties of the coating and substrate. They are given in Ref. [5].

The only unknown in Eq. (1) is G_{cc} or the toughness of the coating. By fitting experiments for crack density as a function of bending strain to Eq. (1), it is possible to determine the toughness of the coating. The bending strain here is defined as the outer-surface strain on the equivalent homogeneous beam. It can be derived from bending moment using

$$\varepsilon_b = \frac{MB}{2E_{0b}I} \quad (2)$$

where M is the constant bending moment in the central span of the four-point bending specimen, $I = WB^3/12$ is the bending moment of inertia of the full beam and E_{0b} is the effective bending modulus of the composite beam; It can be written as [6]:

$$E_{0b} = \frac{E_c I_c + E_s I_s}{I} \quad (3)$$

where I_c and I_s are the bending moments of inertia for the coating and substrate layers about the neutral axis. By the parallel axis theorem, I_c and I_s are:

$$I_c = \frac{Wt_c^3}{12} + Wt_c \left(\frac{t_s}{2} + z_N \right)^2 \quad \text{and} \quad I_s = \frac{Wt_s^3}{12} + Wt_s \left(\frac{t_c}{2} - z_N \right)^2 \quad (4)$$

Here t_s is the thickness of the substrate and z_N is the location of the neutral axis which is given by [6]:

$$z_N = \frac{t_s t_c (E_s - E_c)}{2 E_c t_c + E_s t_s} \quad (5)$$

For a total force of P (or a force of $P/2$ at each loading point), the constant moment is given by

$$M = \frac{PS}{2} \quad (6)$$

where S is the central span between loading points.

3. Results

3.1. Coating A on Several Substrates

Experimental results for Coating A with a thickness of $t_c = 0.114$ mm (4.5 mils) on a PC substrate with a thickness of $t_s = 5.79$ mm (228 mils) are given in Fig. 1. The specimens were baked at 110°C for various amounts of time. For baking times of 6 hours or less, very few coating cracks formed and the experimental results did not conform to the predictions of Eq. (1). For longer baking times, more cracks formed and the experimental results matched reasonably well to the fracture model of Eq. (1). By varying G_{cc} we determined that coating fracture toughness for Coating A on PC was $G_{cc} = 2700, 1600, 1100,$ and 800 J/m² for baking times of 12, 24, 48, and 96 hours, respectively. Thus the toughness significantly decreased as the baking time got longer.

All experiments required high strains to get the formation of many cracks. The load-displacement curves did become non-linear before the end of each test. The initial cracks formed in the linear-elastic region while the later cracks formed in the nonlinear-elastic region. The analysis from Ref. [5] assumes linear elastic components. It is the only analysis we had and thus we used it without any attempt to account for non-linear effects. Note also, that the plotted bending strain is the *maximum* strain on the outer surface of a specimens. Most of the specimen actually sees lower strain and the coating effectively sees lower strain because the cracks release the surface strain. We did try tensile experiments on the coated specimens. The tensile experiments did not show significant cracking until there was substantially more nonlinear deformation than in the bending tests. We suggest the bending specimen is the preferred specimen for studying cracking of coatings.

There were systematic deviations between theory and experiment at low crack density. The theory (smooth curves in Fig. 1) always predicts that the crack density rapidly increases soon after the first coating crack. Physically, this situation corresponds to isolated coating cracks. When the first crack forms, it will release the stresses in the coating near that crack surface. But, moving away from that isolated crack, the stresses will soon return to the far-field stress state; in other words the stresses will soon not be perturbed by the presence of the first crack. Because these unperturbed stresses are essentially the same stresses that caused the first crack to form, new cracks will form immediately after the first crack forms. The cracks will continue forming until the cracks get close enough that their stress fields begin to interact. This failure scenario assumes the entire structure is homogeneous or that the critical conditions for all locations in the coating are identical. In real specimens there will inevitably be heterogeneities, such as defects in the coating and defects on the substrate surface, that cause the local toughness to vary. The first cracks will form at local areas of low toughness, but similar stresses away from these cracks will not immediately cause other cracks. It will require additional strain to cause additional cracks to form. In other words, material heterogeneity will cause the crack density to rise slower than predicted by a homogeneous-toughness theory. Similar observations were made about the related multiple crack problem of matrix microcracking in composite laminates [7–9].

Rather than abandon the fracture mechanics interpretation of the experiments in Eq. (1), we claim that deviations at low strain are a measure of the variability of the toughness properties of the coating. The deviations from the theory naturally decrease at higher strain because the stress states from neighboring cracks begin to interact. At low crack density, the stresses throughout the coating are fairly uniform (except near the few existing cracks). Thus, all areas of low toughness will see similar stresses and the coating is free to crack at any existing low-toughness sites. In contrast, at high crack density, the stress states from neighboring cracks will interact causing only those areas midway between existing cracks to be sites of high stress and likely sites for formation of the next crack. In general, these midway sites will not correspond to weak-link areas of low toughness, but rather will reflect a more uniform or *average* toughness for the coating. When fitting to experimental results, we emphasized the higher crack density results. The calculated G_{cc} 's thus reflect an average *in situ* fracture toughness for the coating. The magnitude of the deviations at low crack density reflect the variability of G_{cc} in the specimen. The results in Fig. 1 indicate that both the average toughness and the toughness variability decreased as the baking time increased.

The theoretical predictions in Fig. 1 all show a region of negative slope that predicts the strain decreases while the crack density increases. These negative slope regions correspond to a real mechanical effect where the energy release rate increases slightly as the cracks begin to approach each other before eventually decreasing as the cracks get even closer. Some plots in Ref. [5] show an elevated energy release rate for coatings on polymeric substrates at crack densities of about 0.5 mm^{-1} that correspond to the negative slope regions in Fig. 1. In real experiments with monotonically increasing strain, it is not possible for experiments to follow the negative slopes of the predictions. Instead, the *prediction* curves imply that after the initiation of cracking, the crack density should rise very rapidly. Ignoring the statistical effects discussed above, the crack density should rise vertically following an extrapolation of the initial vertical rise until it reintersects the prediction curve. Once the vertical rise intersects the prediction curves, the rate of increase in crack density should slow down. The *saturation* of crack density corresponds to a drop in energy release rate due to the formation of the next crack as the cracks get close together.

Because all coatings tested in this paper were baked at elevated temperature before testing at room temperature, there were probably some residual stresses in the coatings. The analysis in Ref. [5] does account for residual stresses; from Eq. (1) it can be seen that residual stresses only enter the second term and thus cause a linear shift in ε_b proportional to the magnitude of $\Delta\alpha\Delta T$. To be able to account for residual stresses, however, one needs an experimental result for the level of residual stresses, or equivalently for $\Delta\alpha\Delta T$. We did not measure either $\Delta\alpha$ or ΔT ; thus we ignored residual stresses in all analyses. Inclusion of residual stresses would not affect to quality of the fits between experiment and theory because for any fit that ignores residual stresses, we could construct a nearly identical fit that includes residual stresses but uses a different value of G_{cc} . In other words, the only effect of including residual stresses would be alter the final value of G_{cc} — G_{cc} would be higher if $\Delta\alpha\Delta T < 0$ and lower if $\Delta\alpha\Delta T > 0$.

Experimental results for Coating A with a thickness of $t_c = 0.153 \text{ mm}$ (6 mils) on a steel substrate with a thickness of $t_s = 3.18 \text{ mm}$ (125 mils) are given in Fig. 2. By using Eq. (1) and varying G_{cc} we determined that coating fracture toughness for Coating A on steel was $G_{cc} = 260, 175, 110,$ and 60 and 45 J/m^2 for baking times of 6, 12, 22, 70, and 369 hours, respectively. Thus the toughness significantly decreased as the baking time got longer.

The results for Coating A on steel were similar to the results on PC in that the toughness decreased with baking time and that there were deviations between theory and experiment at low crack density. The results on steel were different, however, because the measured toughnesses were more than an order of magnitude lower at comparable baking times. We suggest the steel substrate restrained the coating preventing large deformation around new crack surfaces. This limitation of deformation could cause a much lower toughness. In other words, the toughness of a coating is an *in situ* property that depends on the properties of the substrate. The theoretical curves predict that there is less saturation in cracking on steel substrates than on PC substrates for crack densities below 1.0 mm^{-1} . This prediction is consistent with experimental results, but no specimens on steel substrates reached crack densities of 1.0 mm^{-1} . In fitting the Coating A/Steel results, we emphasized the vertical rise section after the initial slower rise at low crack density. The fit toughnesses thus represent *average in situ* toughness results.

The analysis for Coating A on steel also ignored residual stresses, which may account for part of the substrate effect on coating toughness. Our best efforts to estimate the contribution of residual stresses, however, showed that residual stresses can not account for entire reduction in toughness. For polymeric

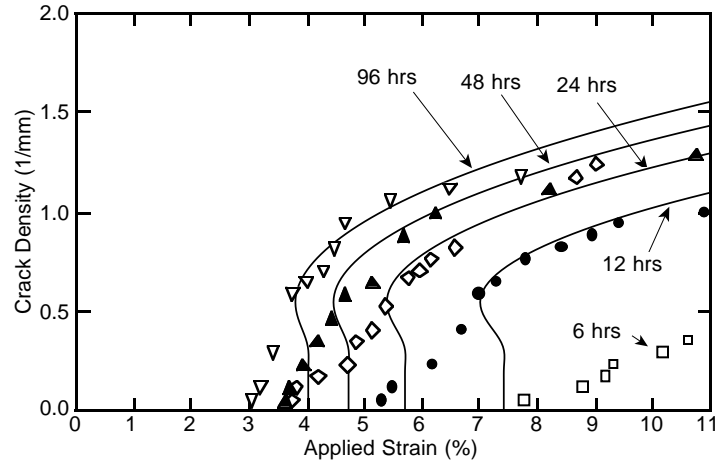


Fig. 1. Coating crack density as a function of bending strain, ε_b , during four-point bending tests with Coating A ($t_c = 4.5$ mils) on a PC ($t_s = 228$ mils) substrate. The data are for specimens that were baked for various amounts of time at 110°C . The smooth curves are fits to Eq. (1) with $G_{cc} = 2700, 1600, 1100,$ and 800 J/m^2 for baking times of 12, 24, 48, and 96 hours, respectively.

coatings on polymer substrates, we estimated that $\Delta\alpha$ is small and thus residual stresses have very little effect on G_{cc} . For polymeric coatings on steel substrates we suggest $\Delta\alpha \sim 40 \times 10^{-6} \text{ }^\circ\text{C}^{-1}$ and ΔT is no larger than -100°C ; these estimates imply $\Delta\alpha\Delta T \sim -0.4\%$. From the shifts of the curves in Fig. 2 as a function of strain, we can estimate that $\Delta\alpha\Delta T \sim -0.4\%$ would cause the *true* G_{cc} to be $40\text{--}50 \text{ J/m}^2$ higher than the quoted G_{cc} that ignores residual stresses. This magnitude increase in G_{cc} can not account for the order of magnitude difference between *in situ* toughness on PC and steel substrates.

Experimental results for Coating A with a thickness of $t_c = 0.153 \text{ mm}$ (6 mils) on an ABS substrate with a thickness of $t_s = 6.57 \text{ mm}$ (259 mils) are given in Fig. 3. The one specimen tested was baked for 100 hrs at 60°C . The experimental results did not conform well to the predictions of Eq. (1). Perhaps the lower baking time for ABS specimens prevented the coating from fully curing and the results are therefore similar to the 6 hr results on PC (see Fig. 1). It is also possible that the paint delaminated and thus could not be interpreted by a theory that assumes multiple cracking. By fitting various portions of the curve we

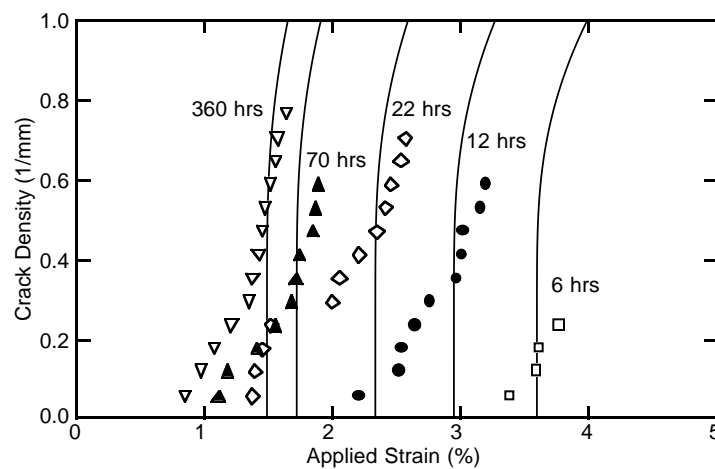


Fig. 2. Coating crack density as a function of bending strain, ε_b , during four-point bending tests with Coating A ($t_c = 6$ mils) on a steel ($t_s = 125$ mils) substrate. The data are for specimens that were baked for various amounts of time at 110°C . The smooth curves are fits to Eq. (1) with $G_{cc} = 260, 175, 110,$ and 60 and 45 J/m^2 for baking times of 6, 12, 22, 70, and 360 hours, respectively.

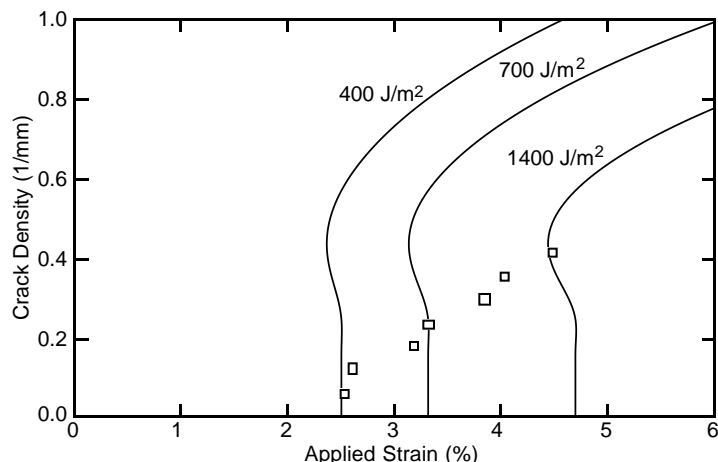


Fig. 3. Coating crack density as a function of bending strain, ε_b , during four-point bending tests with Coating A ($t_c = 6$ mils) on an ABS ($t_s = 259$ mils) substrate. The data are for a specimen baked for 100 hrs at 60°C . The smooth curves are several predictions of Eq. (1) using various values for G_{cc} .

derived a crude estimate for toughness of Coating A on ABS. The toughness could range from $G_{cc} = 400$ to 1400 J/m^2 depending on whether one fits to the early cracks or the later cracks. This range in toughness is similar to the toughness results on PC and much higher than the toughness results on steel.

3.2. Coatings B and C on PC Substrates

Both Coating B and Coating C were tested on the same geometry PC substrate ($t_s = 5.79$ mm or 228 mils) as that used for the Coating A experiments (see Fig. 1). The results for Coating B with a thickness of $t_c = 0.102$ mm (4 mils) and Coating C with a thickness of $t_c = 0.171$ mm (6.75 mils) are given in Fig. 4. The toughness as a function of baking time at 110°C for Coating B was determined using Eq. (1) to be $G_{cc} = 2800, 2000, \text{ and } 1500 \text{ J/m}^2$ for baking times of 12, 24, and 48 hours, respectively. The toughness for Coating C after 10 hours of baking was determined to be $G_{cc} = 2600 \text{ J/m}^2$. All aspects of the results for Coatings B and C on PC are similar to the results for Coating A on PC. The toughness decreased with baking time. The magnitude of the toughnesses were high — as they were for Coating A on polymeric substrates. There were systematic deviations between experiment and theory at low strains.

3.3. Coating C on Steel Substrates

The results of Coating C on steel substrates were essentially identical to the results of Coating A on steel. Similar to the results in Fig. 2 the Coating C results had some initial curvature, followed by a rapid rise in crack density, and no evidence of saturation before the test was stopped. By fitting the rapid rise portion of each curve the toughness was determined to be $G_{cc} = 40, 40, 36, \text{ and } 29 \text{ J/m}^2$ for baking times of 6, 12, 24, and 63 hours, respectively. Again, the coating toughness on a steel substrate was more than one order of magnitude lower than it was on a polymeric substrate.

The results in Fig. 5 show the analysis of two different specimens with Coating C on a steel substrate ($t_s = 3.18$ mm (125 mils)) with identical baking times. The only difference between the two specimens were the coating thicknesses — one coating had a thickness of $t_p = 0.051$ mm (2 mils) while the other had a thickness of $t_p = 0.152$ mm (6 mils). By fitting to the rapid rise portion of the 2 mil thick coating specimen to Eq. (1) the coating toughness was estimated to be $G_{cc} = 24 \text{ J/m}^2$. When this toughness was used to predict the results for the thicker 6 mil coating, the predictions were qualitatively correct. In particular, the fracture analysis correctly predicts that cracks form sooner when the coating is thicker. Quantitatively, however, the fracture analysis over predicts the shift to lower strain. The thicker coating acts like it is tougher than the thinner coating; a fit to the rapid rise portion of the 6 mil thick coating results gives a $G_{cc} = 40 \text{ J/m}^2$. Previously, we suggested that the dramatically higher *in situ* toughness for coatings on

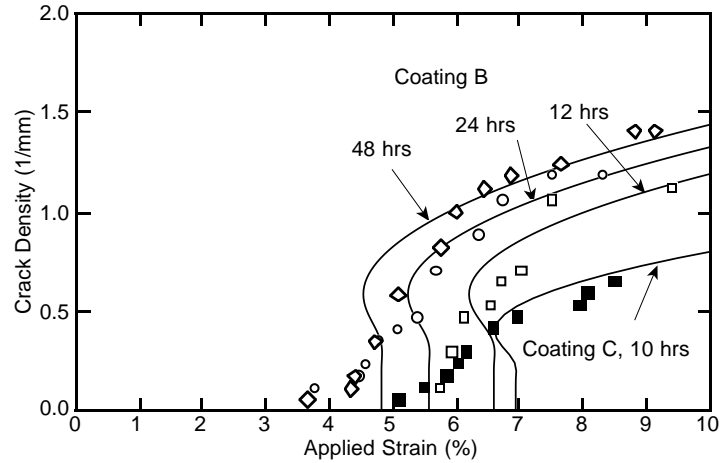


Fig. 4. Coating crack density as a function of bending strain, ε_b , during four-point bending tests with Coating B ($t_c = 4$ mils) (unfilled symbols) and Coating C ($t_c = 6.75$ mils) (filled symbols) on a PC ($t_s = 228$ mils) substrates. The data are for specimens that were baked for various amounts of time at 110°C . The smooth curves are fits to Eq. (1). The fits for Coating B gave $G_{cc} = 2800, 2000,$ and 1500 J/m^2 for baking times of 12, 24, and 48 hours, respectively. The fit for Coating C gave $G_{cc} = 2600 \text{ J/m}^2$ for 10 hours of baking.

polymer substrates *vs.* steel substrates is a consequence of the reduction in constraint provided by polymer substrates *vs.* steel substrates. Similarly, steel substrates may provide less constraint to thicker coatings than to thinner coatings. Thus, the slightly higher toughness of the 6 mil coating may be a real observation of changes in *in situ* toughness caused by specimen geometry.

Notice that the raw experimental data show that thicker coatings crack sooner than thinner coatings. Without a fracture analysis, one might conclude the steel substrates embrittle thicker coatings more than thinner coatings. With a fracture analysis, however, we can determine that the *in situ* toughness actually *increased* as the coating thickness increased. Even though the toughness increased, the cracks formed sooner in thicker coatings because each crack released more energy than the corresponding crack in a thinner coating. Thus, the increase in amount of energy released due to crack formation in thicker coatings was larger than the increase in *in situ* toughness.

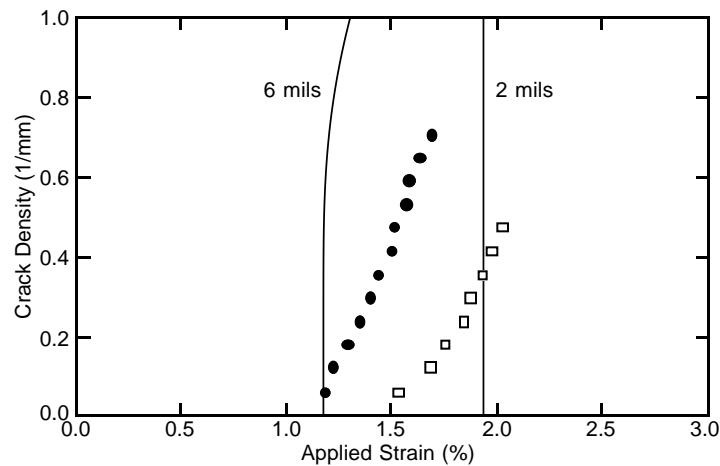


Fig. 5. Coating crack density as a function of bending strain, ε_b , during four-point bending tests with two different thicknesses of Coating C ($t_c = 2$ mils and $t_c = 6$ mils) on steel ($t_s = 125$ mils) substrates. Both smooth curves are predictions of Eq. (1) assuming the coating toughness is $G_{cc} = 24 \text{ J/m}^2$.

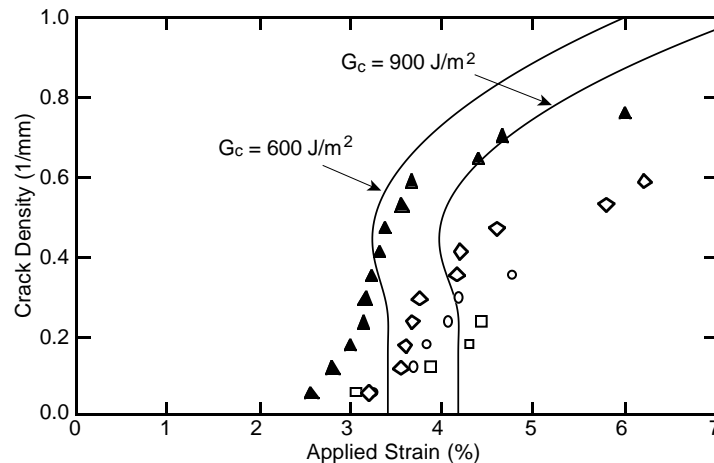


Fig. 6. Coating crack density as a function of bending strain, ε_b , during four-point bending tests with Coating D ($t_c = 6$ mils) on a PC ($t_s = 228$ mils) substrate. The unfilled symbols are for specimens that were dried for less than 10 days; the filled symbols are for a specimen that was dried for 10 days; drying was done at 60°C . The smooth curves are fits to Eq. (1) with $G_{cc} = 900$ or 600 J/m^2 for drying times of < 10 or 10 days, respectively.

3.4. Coating D on PC Substrates

Coating D was physically different than Coatings A, B, and C. Coating D “dried” by removal of solvents while Coatings A, B, and C were cured by baking. Coating D contains PMMA resin and has been used in the past for automotive finishes characterized and brittle-lacquer finishes. Experimental results for Coating D with a thickness of $t_c = 0.152$ mm (6 mils) on a PC substrate with a thickness of $t_s = 5.79$ mm (228 mils) are given in Fig. 6. The specimens were dried at 60°C for various amounts of time. For drying times of less than 10 days (unfilled symbols), there was very little change in cracking properties and the fit to Eq. (1) was only qualitative. By fitting to the rapid rise portion of the curve, we estimated the toughness for drying less than 10 days to be $G_{cc} = 900$ J/m^2 . After drying for 10 days, the cracking data fit Eq. (1) better; from a best-fit analysis, the toughness dropped to $G_{cc} = 600$ J/m^2 . The toughness of Coating D on PC was comparable to or lower than the *in situ* toughness of the most aggressively baked Coatings A, B, and C.

We also did experiments with Coating D on ABS and Noryl substrates. The results were similar to the result in Fig. 3 in that they could not be fit well to Eq. (1). In general, the cracking process saturated much faster than predicted by theory. Our best estimate of toughness for Coating D on ABS or Noryl was about $G_{cc} = 500$ J/m^2 . This toughness is comparable in magnitude to Coating D on PC and higher than typical toughnesses for coatings on steel substrates.

4. Discussion and Conclusions

Most experimental results for specimens with PC or steel substrates conformed reasonably well to the finite fracture mechanics predictions of Eq. (1). There were systematic deviations between theory and experiment, most notably at low crack density where the crack density typically rose more slowly than predicted. One could cite these deviations as evidence that the fracture mechanics analysis is not correct. Instead, we claim the fracture mechanics analysis is correct and that the deviations represent real variations in coating properties. In effect, the fracture toughness G_{cc} can be considered as being a statistical quantity. Variations in G_{cc} cause experimental results to spread out relative to the predictions of Eq. (1) which are based on a single-valued G_{cc} . At high crack density, the experimental results naturally become less sensitive to statistical variations in G_{cc} and the fits between experiment and theory correspondingly become better.

The recommended fracture mechanics experiment for determining the *in situ* fracture toughness of a coating is thus to load a coated specimen in four-point bending and record the number of coating cracks as a function of applied bending strain. This experimental data can be fit to Eq. (1) to determine G_{cc} . This fitting process should emphasize the middle and high crack density results to determine an *average* G_{cc} .

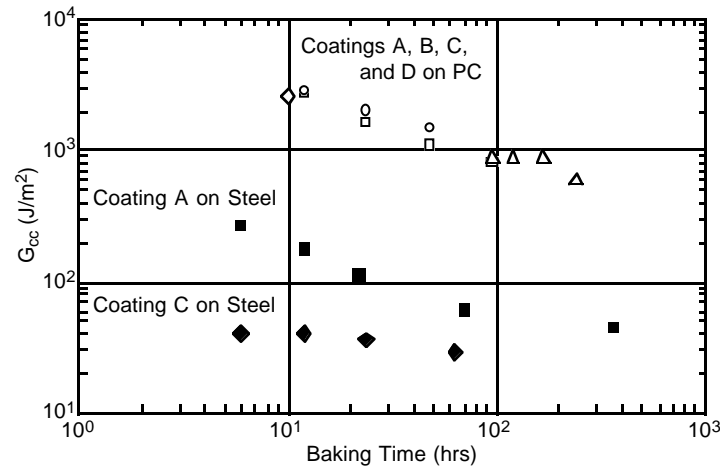


Fig. 7. Coating fracture toughness as a function of baking time for Coatings A, B, C, and D on PC (unfilled symbols) and Coatings A and C on steel (filled symbols).

Some conclusions about the variability in G_{cc} can be drawn by observing discrepancies between theory and experiment at low crack density.

Coating toughness, G_{cc} , is not a property only of the coating. Instead, G_{cc} is a system property or an *in situ* toughness of the coating. It depends on the substrate properties as well as the coating properties and also depends on the thickness of the coating. All experimental results for G_{cc} presented here are plotted in Fig. 7 (a log-log plot is used to best show all results on a single plot). There is a large substrate effect. The *in situ* toughnesses for these polymeric coatings was more than an order of magnitude lower on a steel substrates than they were on a PC substrates. The results for Coating A on PC (unfilled squares) and on steel (filled squares) and the results for Coating C on PC (unfilled diamond) and on steel (filled diamonds) clearly show this substrate effect. We suggest this reduced toughness is caused by the extra constraint provided by steel substrates *vs.* PC substrates.

Even on the same substrate, the *in situ* toughness of coatings depends on the coating thickness. Based on constraint arguments, we expect that the coating toughness will increase as the coatings get thicker. This expectation agrees with experimental results for Coating C on steel substrates. Paradoxically, even though the toughness increases as the coatings get thicker, thicker coatings may still crack sooner than thinner coatings. Such behavior can be explained by the theoretical result that the total energy released due to formation of a single crack also increases as the coating thickness increases [5]. Whenever the increase in energy release rate due to thickness is larger than the increase in toughness due to thickness, thicker coatings will crack sooner than thinner coatings. This situation occurs, for example, for Coating C on steel substrates.

Acknowledgment

This work was supported by a grant from the Mechanics of Materials program at the National Science Foundation (CMS-9713356). All materials and some additional support were provided by the duPont company under the direction of Dr. Paul McGonigal.

References

1. Nairn, J. A. and S. R. Kim, A Fracture Mechanics Analysis of Multiple Cracking in Coatings. *Eng. Fract. Mech.*, 1992, **42**, 195–208.
2. Kim, S. R., *Fracture Mechanics Approach to Multiple Cracking in Paint Films*, M.S. Thesis, University of Utah, 1989.
3. Kim, S. R., *Understanding Cracking Failures of Coatings: A Fracture Mechanics Approach*, Ph.D. Thesis, University of Utah, 1993.
4. Hsieh, A. J., P. Huang, S. K. Venkataraman, and D. L. Kohlstedt, Mechanical Characterization of Diamond-Like Carbon (DLC) Coated Polycarbonates. *Mat. Res. Cos. Symp. Proc.*, 1993, **308**, 653–658.

5. Kim, S. R. and J. A. Nairn, Fracture Mechanics Analysis of Coating/Substrate Systems: I. Analysis of Tensile and Bending Experiments. *Engr. Fract. Mech.*, 2000, **in press**.
6. Crandall, S. H., Dahl, N. C., and Lardner, T. J., *An Introduction to the Mechanics of Solids*, McGraw-Hill, New York, 1978.
7. Liu, S. and J. A. Nairn, The Formation and Propagation of Matrix Microcracks in Cross-Ply Laminates During Static Loading. *J. Reinf. Plast. & Comp.*, 1992, **11**, 158–178.
8. Nairn, J. A., S. Hu, and J. S. Bark, A Critical Evaluation of Theories for Predicting Microcracking in Composite Laminates. *J. Mat. Sci.*, 1993, **28**, 5099–5111.
9. Nairn, J. A. and S. Hu, Micromechanics of Damage: A Case Study of Matrix Microcracking. *Damage Mechanics of Composite Materials*, ed., Ramesh Talreja, Elsevier, Amsterdam, 1994, 187–243.